



Age-related functional brain changes in *FMR1* premutation carriers

Stephanie S.G. Brown^{a,*}, Shinjini Basu^b, Heather C. Whalley^a, Peter C. Kind^b,
Andrew C. Stanfield^a

^a Patrick Wild Centre, Division of Psychiatry, School of Molecular and Clinical Medicine, University of Edinburgh, Royal Edinburgh Hospital, Edinburgh EH10 5HF, UK

^b Patrick Wild Centre, Centre for Integrative Physiology, School of Biomedical Sciences, University of Edinburgh, Hugh Robson Building, 15 George Square, Edinburgh EH8 9XD, UK

ARTICLE INFO

Keywords:

Fragile X premutation
FXTAS
fMRI
Neuroimaging
Neurodegeneration

ABSTRACT

The *FMR1* premutation confers a 40–60% risk for males of developing a neurodegenerative disease called the Fragile X-associated Tremor Ataxia Syndrome (FXTAS). FXTAS is a late-onset disease that primarily involves progressive symptoms of tremor and ataxia, as well as cognitive decline that can develop into dementia in some patients. At present, it is not clear whether changes to brain function are detectable in motor regions prior to the onset of frank symptomatology. The present study therefore aimed to utilize an fMRI motor task for the first time in an asymptomatic premutation population.

Premutation carriers without a diagnosis of FXTAS ($n = 17$) and a group of healthy male controls ($n = 17$), with an age range of 24–68 years old, were recruited for this cross-sectional study. This study utilized neuroimaging, molecular and clinical measurements, employing an fMRI finger-tapping task with a block design consisting of sequential finger-tapping, random finger-tapping and rest conditions. The imaging analysis contrasted the sequential and random conditions to investigate activation changes in response to a change in task demand. Additionally, measurements were obtained of participant tremor, co-ordination and balance using the CATSYS-2000 system and measures of *FMR1* mRNA were quantified from peripheral blood samples using quantitative real-time PCR methodology.

Premutation carriers demonstrated significantly less cerebellar activation than controls during sequential versus random finger tapping ($FWE_{\text{corr}} < 0.001$). In addition, there was a significant age by group interaction in the hippocampus, inferior parietal cortex and temporal cortex originating from a more negative relationship between brain activation and age in the carrier group compared to the controls ($FWE_{\text{corr}} < 0.001$).

Here, we present for the first time functional imaging-based evidence for early movement-related neurodegeneration in Fragile X premutation carriers. These changes pre-exist the diagnosis of FXTAS and are greatest in older carriers suggesting that they may be indicative of FXTAS vulnerability.

1. Introduction

It is estimated that approximately 1 in 250–810 males in the general population carry the *FMR1* premutation; a genetic status conferred by an expansion of the 5' untranslated CGG repeat region of the *FMR1* gene from < 55 repeats to between 55 and 200 repeats (Rifé et al., 2003; Sorensen et al., 2013). Up to 45 repeats is considered to be within the normal range and 45–55 repeats is considered to be an intermediate expansion. CGG repeat regions exceeding 200 usually become methylated, and as such prevents transcriptional regulation, silencing the *FMR1* gene. This is known as a full mutation, causing Fragile X Syndrome, which is functionally and pathologically separate from disorders linked to the Fragile X premutation (Tassone and Berry-Kravis, 2010).

Until relatively recently it was believed that carriers of the *FMR1*

repeat expansion were phenotypically unaffected. However, research carried out over the last two decades has revealed that carriers of the *FMR1* premutation are at risk of developing a late onset neurological condition called Fragile X-associated Tremor Ataxia Syndrome (FXTAS), which is characterised by progressive core symptoms of tremor, ataxia and cognitive decline. Males have a 40–60% chance of developing FXTAS, whereas females are at lower risk, with a 8–16% chance of developing the disease (Jacquemont et al., 2004; Hall et al., 2005). The clinical presentation of FXTAS usually begins with subtle cognitive decline, especially in executive function and working memory, which develops into full dementia in about 40% of male patients (Bourgeois et al., 2007). Motor symptoms usually include tremor, ataxia and inability for tandem gait. Parkinsonism can also occur in some individuals with FXTAS, as well as peripheral neuropathy,

* Corresponding author.

E-mail address: s0935170@sms.ed.ac.uk (S.S.G. Brown).

autonomic dysfunction and endocrine dysfunction (Loesch et al., 2005; Berry-Kravis et al., 2007; Wang et al., 2013). In addition to these neurological symptoms, a diagnosis of FXTAS requires one or more radiological findings (Hall et al., 2016), including global brain atrophy, increased T2 signal intensity at the middle cerebellar peduncles (known as the MCP sign) and thinning of the corpus callosum (Filley et al., 2015; Brunberg et al., 2002). Evidence suggests that the pathology of FXTAS may be driven primarily by a two to eight fold increase in *FMR1* mRNA (Li and Jin, 2012; Garcia-Arocena and Hagerman, 2010). Intracellular inclusions in multiple brain cell types are a pathological hallmark of FXTAS, and in both FXTAS models and patient brain slices these inclusions have been shown to contain *FMR1* mRNA. It is theorised that excess of *FMR1* mRNA causes sequestration of RNA binding proteins, forming aggregates and causing cell-wide disruption, resulting in oxidative stress and eventual apoptosis (Tassone et al., 2000; Hagerman and Hagerman, 2013).

Progressive motor symptoms are therefore a core feature of FXTAS, with clinical signs of the condition only rarely manifesting before 50 years old. It is however possible that significant neurodegeneration is already occurring before clinical features of motor dysfunction emerge. In order to determine whether this is indeed the case we set out to investigate whether subtle differences in brain activation during motor function can be elicited using functional magnetic resonance imaging (fMRI), even in premutation carriers without a diagnosis of FXTAS. We utilized a finger tapping task which contained both sequential and random finger tapping components. Compared to planned sequential tapping, random, choice-driven tapping is known to elicit higher levels of activation in classical motor regions and rely more upon regions of higher cognitive functioning, such as the dorsolateral prefrontal cortex (Gountouna et al., 2010). To the authors' knowledge, there have been no previous neuroimaging studies which have examined these functions in premutation carriers, although other studies have investigated brain changes in carriers without FXTAS. A systematic review of neuroimaging studies in premutation carriers provides an overview of these findings (Brown and Stanfield, 2015), including a reduction in brainstem volume in carriers without FXTAS (Cohen et al., 2006), significant correlation between hippocampal volume and anxiety measures in female carriers without FXTAS (Adams et al., 2010), significant elevations in axial and radial diffusivities in male carriers without FXTAS (Hashimoto et al., 2011) and significantly lower BOLD response at the right temporoparietal junction compared to controls during a working memory task in a group of male and female asymptomatic carriers (Kim et al., 2014). Finger-tapping studies in other neurodegenerative disorders, such as Huntington Disease (Bartenstein et al., 1997; Kloppel et al., 2009), Spinocerebellar Ataxia Type 3 (Duarte et al., 2016; Cleary and Ranum, 2014) and Parkinson Disease (Lewis et al., 2011) have demonstrated impaired functional activity in motor regions and dysregulation of compensatory activity, in particular during conditions with higher demand. The finger-tapping task for this study was therefore designed to involve various levels of cognitive and motor complexity using sequential and random tapping conditions, with the intention of contrasting these two conditions during the imaging analysis to isolate regions of changing activations in response to task demands.

The primary aim of this study was therefore to determine whether, compared to controls, differences in brain activation are apparent during motor function in premutation carriers who do not have a diagnosis of FXTAS. The secondary aim was to use this cross-sectional sample to look for preliminary evidence of progressive changes to brain function in premutation carriers by comparing the relationship between age and brain function in premutation carriers and controls. It was hypothesised that differences in brain activation in motor regions, such as the premotor cortex, supplementary motor area and the cerebellum, would be seen between controls and premutation carriers without FXTAS, in addition to differences in other regional involvement of compensatory mechanisms (Lewis et al., 2011; Duarte et al., 2016;

Table 1Summary data of participant age, IQ, *FMR1* mRNA level and CATSYS-2000 performance.

Participant summary data				
	Control mean	Control SD	Carrier mean	Carrier SD
Age (years)	47.6	12.9	50.4	15.1
Verbal IQ	112.8	13.5	111.1	15.8
Non-verbal IQ	117.4	7.7	108.1	13.7
Composite IQ	116.4	9.1	110.4	14.9
<i>FMR1</i> mRNA level	1.9×10^{-6}	1.9×10^{-5}	3.3×10^{-6}	3.3×10^{-5}
Tremor index	43	7.2	32.5	10.6
Co-ordination index	131.1	15.4	108.8	19.1
Balance index	171.9	15.6	173.0	13.0

Bartenstein et al., 1997; Minkova et al., 2015; Murta et al., 2016). Finally, we also predicted that the degree of change in brain activation in carriers may show an association with levels of *FMR1* mRNA and extent of movement symptoms.

2. Materials and methods

2.1. Participants and recruitment

Male premutation carriers without FXTAS and a group of age-matched healthy male controls were recruited through the Fragile X Society, UK. Invitation letters were sent to 1000 individuals of known Fragile X families across the UK via the existing database held by the Fragile X Society charitable association. Eligible participant age range was between 20 and 70 years. Potential participants falling out with an age range of 20–70 years, with a diagnosis of FXTAS or from a Fragile X family but without a genetic diagnosis of the premutation were excluded. All participants had normal or corrected-to-normal vision. All participants underwent genetic testing for *FMR1* CGG repeat length (Table 1). All participants gave fully informed written consent and were screened for MRI eligibility and safety. The study was approved by South East Scotland Research Ethics Committee, NHS Lothian.

2.2. Imaging methods

All MRI data was acquired using a 3.0 Tesla Siemens MRI scanner using an 8 channel head coil. For the acquisition of functional images the TR was 1560 ms, the TE (echo time) was 26 ms, the flip angle was 66°, the FOV (field of view) was 220 mm, slice thickness was 5 mm and slice number per volume was 26. Slice order was interleaved and bottom up in the axial orientation. Each participant also underwent a T1-weighted magnetization prepared rapid acquisition gradient echo (MPRAGE) sequence, in addition to fMRI sequences, for the purpose of image preprocessing. For the MPRAGE acquisition the TR was 2300 ms, the TE was 2.98 ms, the flip angle was 9°, the FOV was 256 mm, slice thickness was 1 mm and slice number per slab was 160. Structural and functional images were acquired during the same scanning session.

The finger-tapping task designed and used for this study utilized a block design and consisted of three conditions, based on Gountouna et al., 2010. In the sequential tapping condition, participants were asked to tap their thumbs and index fingers on trigger buttons in a predetermined sequence in time with a flashing symbol. In the random tapping condition, participants were asked to tap their thumbs and fingers on the trigger buttons in time with the flashing symbol in a random order of their choosing. The final condition consisted of a flashing fixation cross, where participants were asked to rest and watch the screen (Fig. 1). The purpose of this fixation/rest condition was to allow a control condition minimising possible noise from visual stimulus. The flashing symbol appeared once every second, for a duration of 0.5 s. Each condition block had a total duration of 30 s, including a 2 second prompt screen, and was repeated 4 times during the task. This

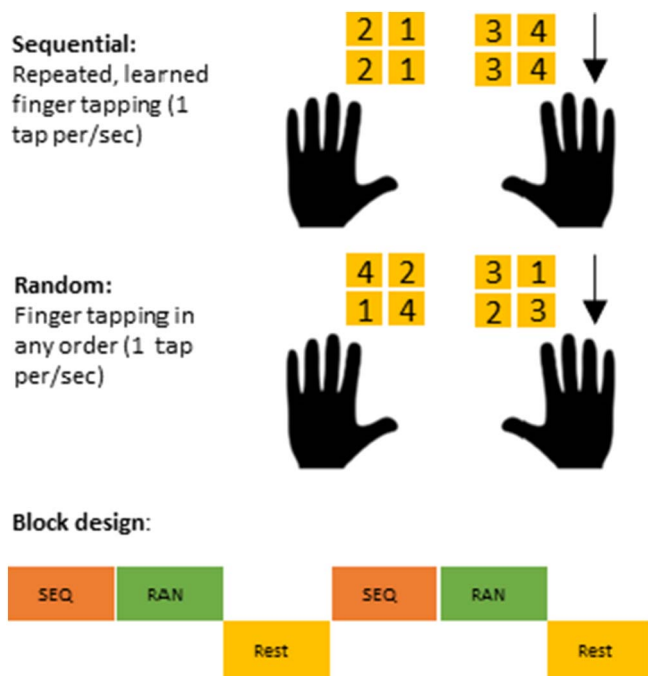


Fig. 1. Finger-tapping task behavioural conditions and block design.

functional task was programmed using Presentation™ software, and was visually presented to participants using goggles that fit onto the scanner head coil. All participants were given instructions to the task prior to the scan, and were given practice time to memorise the tapping sequence for the sequential condition.

2.3. fMRI analysis

Statistical analysis on fMRI data was carried out using Statistical Parametric Mapping software (SPM12) (Wellcome Department of Clinical Neurology) using standard procedures.

The functional images from all participants were preprocessed using the following steps: 1) images were realigned, estimated (for optimal transformation from individual images to the reference using SPM12 default quality, separation, smoothing, num passes, interpolation, wrapping and weighting parameters) and resliced 2) images were slice timed, adjusting for interleaved and bottom up slice order 3) subsequent images were then coregistered with the source structural image from the T1-weighted MPAGE anatomical scan 4) coregistered images were segmented into grey matter, white matter and CSF outputs 5) segmented (forward deformation) images were normalised to MNI space and 6) finally, normalised images were smoothed with an 8 mm full-width at half maximum (FWHM) Gaussian smoothing kernel.

Movement was controlled for by adding realignment parameters for each participant as a multiple regressor into the first level model. For the first-level analysis, the onsets and durations of the conditions were modelled, excluding the prompt screen stimuli. The contrast of interest here was between the sequential and random conditions, as we aimed to focus on brain regions associated with the changes in demand for movement cognition and planning. For the second-level analysis, an explicit mask was derived from an average binarised image created from the combined grey matter and white matter segmented images from all participants and was used to exclude voxel data out-with the brain tissue. Between group analyses were completed using a p threshold value of $p < 0.005$ and significant suprathreshold clusters were defined as FWE corrected $p < 0.05$. Firstly, between group analyses were performed using a two-sample t -test with age as a covariate. A full factorial design was used for a secondary analysis, carried out with age added into the model as a possible interacting variable.

CGG repeat analysis revealed that some individuals in the sample were mosaic or borderline for the full mutation. To ensure this was not causing a bias in the results, a one-way ANOVA of 3 age-matched groups, followed by a Tukey post-hoc test was performed on extracted voxel data from the maximum voxel of the significantly different between group cluster and a univariate analysis of variance was performed on extracted voxel data from the age interaction significant cluster.

2.4. Tremor, balance and co-ordination measurements

Although no participants had frank symptoms of FXTAS, detailed quantification of tremor, balance and co-ordination was conducted to examine for sub-threshold symptomatology using the CATSYS 2000 PC-based test system. This system has previously been used in other studies to establish that carriers without FXTAS exhibit worse co-ordination scores and to generate estimates of age-related prevalence of tremor and ataxia in carriers (Allen et al., 2008; Aguilar et al., 2008). Here, index scores were obtained as standard deviations of normal human performance, as defined by the CATSYS 2000 test battery, with performance indices above 1 being better than normal human performance and indices below 1 being below normal human performance (Danish Product Development Ltd., 1988).

2.5. Molecular measurements

DNA was isolated from blood samples for both control and carrier participants. The assay for CGG repeat length in the *FMR1* gene was carried out using a PCR-only approach based on Triplet Repeat Primed PCR design (AmplideX® PCR/CE *FMR1* reagents).

Whole blood was collected from all participants and processed to isolate total RNA. Total RNA was then reverse transcribed into cDNA, using RT-PCR methodology. RT reactions were performed in 25 μ l aliquots containing 10 μ l of patient total RNA sample, 12.5 μ l $2 \times$ RT buffer and RT enzyme mix (Invitrogen Superscript). RT thermal cycling conditions were as follows: 25 °C for 10 min, 50 °C for 30 min, 85 °C for 5 min and 4 °C for 15 min. 1 μ l of RNase H was subsequently added to each aliquot and the samples were incubated at 37 °C for 20 min. Each sample was then diluted to a cDNA concentration of 6 ng/ μ l. These dilutions were then used to quantify *FMR1* mRNA using quantitative PCR (qPCR). In the present investigation, the *FMR1* amplicon is a 130 bp product and the following primer pair was used: forward primer 5'-AGGCAGTTGGTGCCTTTCT-3', starting at bp185, reverse primer 5'-TTAGTGCGCAGACTCCGAAA-3' starting at bp314. The *FMR1* primer pair was validated (primer efficiency = 101.01%, $R^2 = -0.998$) and aliquots were prepared in triplicate for each sample, with each aliquot containing 0.6 μ l 300 nM forwards primer, 0.6 μ l 300 nM reverse primer, 10 μ l SYBR Green (Qiagen), 11.8 μ l H₂O and 1 μ l 6 ng/ μ l cDNA sample. An additional control was run in triplicate on each plate with cDNA replaced by H₂O. Thermal cycling conditions for the qPCR were as follows: 95 °C for 15 min, (94 °C for 20 s, 59 °C for 30 s and 32 °C for 30 s) \times 35 cycles, then 95 °C for 1 min, 60 °C for 30 s and 90 °C for 30 s.

All *FMR1* mRNA measurements were normalised to 18 sRNA measurements from the samples (average primer efficiency = 91.28%, $R^2 = -0.994$), which were also ran in triplicate on the same qPCR plate as the *FMR1* mRNA probes. All samples underwent qPCR analysis on the same plate as their age-matched counterpart. Carrier *FMR1* mRNA was then additionally normalised to age-matched control.

2.6. Statistical analyses

Imaging analyses are detailed above. Further statistical analyses were carried out in SPSS Statistics 22. A two-tailed t -test was used to discern differences between the premutation and control groups for the tremor, balance and coordination measurements, in addition to the *FMR1* mRNA data. Simple linear regressions were also performed on

extracted raw voxel values from significant clusters against the movement and molecular variables. All significance levels were assumed at $p < 0.05$.

3. Results

3.1. Participants

Male premutation carriers without FXTAS ($n = 17$, mean age 50.4 years, $SD = 15.1$) and a group of age-matched healthy male controls ($n = 17$, mean age 47.6 years, $SD = 12.9$) were recruited for this study. CGG repeat testing revealed that 12 carriers were within the premutation range, 1 carrier was in the intermediate range, 3 carriers were mosaic for repeat size and one carrier was borderline for the full mutation. All control subjects were within the normal CGG repeat length range (Supplementary Table 1). All participants were right handed, apart from one control and two carriers, and all participants had an IQ > 80 , as measured by the KBIT Second Edition Intelligence Test (Pearson). Participant summary data is shown in Table 1.

3.2. Between group imaging results

Between group full factorial analysis revealed that the premutation group had a significantly lower cluster of BOLD response ($FWE_{\text{corr}} < 0.001$, $T = 5.59$) at the bilateral lobules VI of the cerebellum, left lobule V and the left hippocampus (subiculum) compared to controls. The maximum of the cluster was located at $[-12, -36, -12]$ (Fig. 2a).

As analysis of *FMR1* CGG repeat length revealed a number of carriers in the sample to be mosaic or borderline for the full mutation, a third group was created of mosaic and borderline carriers to examine whether they were skewing the imaging results. The groups for the ANOVA analysis were defined as the following: control ($n = 17$), premutation ($n = 13$) and mosaic/borderline carriers ($n = 4$). A statistically significant between group difference in BOLD response at the significant cluster maximum voxel $[-12, -36, -12]$ was identified by one-way ANOVA ($F(2,31) = 14.249$, $p < 0.001$). A Tukey post-hoc test revealed that BOLD response for this cluster was significantly different in controls compared to carriers ($p < 0.001$) and controls compared to mosaic/borderline carriers ($p = 0.026$), but not significantly different between carriers and mosaic/borderline carriers ($p = 0.784$). Representative group means are presented in Fig. 2b.

3.3. Age-related between group imaging results

In the analysis of age related differences, a significant group \times age interaction was seen in a cluster centred in left Brodmann Area (BA) 17 in the primary visual cortex, which extended to the left hippocampus (cornu ammonis), the left inferior parietal cortex and the left temporal lobe ($FWE_{\text{corr}} < 0.001$, $T = 5.22$). The maximum of the cluster is located at $[-26, 2, 36]$ (Fig. 3a). Plotting extracted values from this cluster indicated there was a negative relationship between age and activation in this cluster in the premutation group, while the relationship was positive in the control group. Within group regression analysis revealed both of these relationships to be significant (Table 2).

A univariate analysis of variance was also carried out on this significant cluster to ensure anomalous CGG repeat lengths were not causing a bias in the imaging results. The groups for the univariate analysis of variance analysis were defined as the following: control ($n = 17$), premutation ($n = 13$) and mosaic/borderline carriers ($n = 4$). A statistically significant group \times age interaction was identified in BOLD response at the significant cluster maximum voxel $[-26, 2, 36]$ ($p < 0.001$), and plotting of group \times age extracted voxel data demonstrates that both the premutation and the mosaic/borderline group differ significantly to controls but not to each other (Fig. 3b).

3.4. Tremor, balance and co-ordination results

Although none of this population of carriers had a diagnosis of FXTAS, the CATSYS-2000 system identified carriers as having significantly worse tremor and co-ordination scores than controls ($p = 0.002$, $p = 0.001$), and balance showed no difference between the groups ($p = 0.931$). Both populations had mean performance indices of better than normal human performance on the co-ordination and balance measurements and below normal human performance on the tremor measurement (Table 1).

3.5. *FMR1* mRNA analysis

Quantitative PCR analysis revealed that the premutation carriers did not have significantly higher levels of *FMR1* mRNA relative to 18 sRNA when measured from peripheral blood samples ($p = 0.3223$) (Fig. 4a). However, normalization of carrier *FMR1* mRNA relative to 18 sRNA to age-matched control data showed that some carriers have up to a 7-fold increase in *FMR1* mRNA when compared directly to an age-matched control (Fig. 4b). To examine again whether the borderline or mosaic carriers were causing anomalies in the data, these individuals were again examined separately from the other premutation carriers.

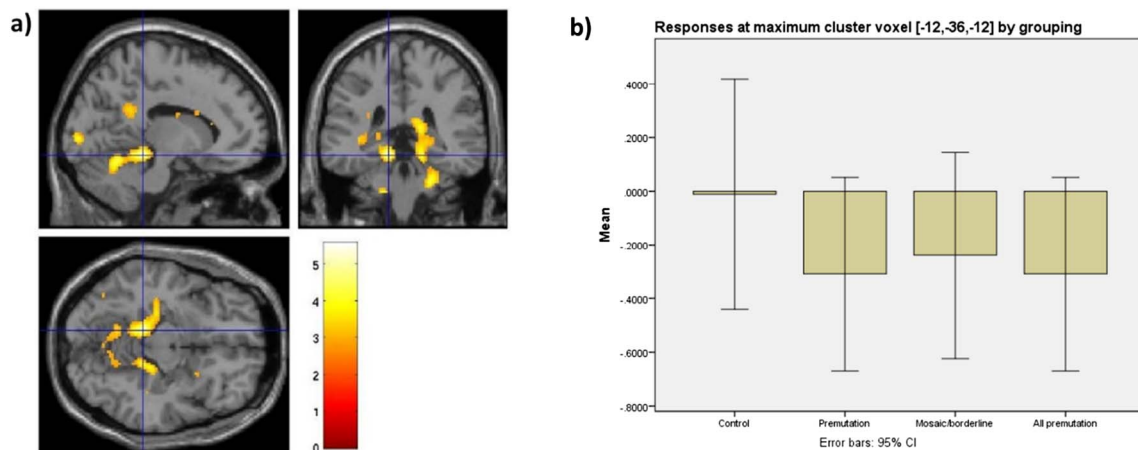


Fig. 2. Between group imaging results a) Premutation group significantly less activated ($FWE_{\text{corr}} < 0.001$, $T = 5.59$) at the bilateral lobules VI of the cerebellum, left lobule V and the left hippocampus (subiculum) in the sequential $>$ random condition contrast. Cluster co-ordinate of maximum voxel: $-12, -36, -12$, $k = 2040$, normalised voxel size: 2 mm^3 b) Mean extracted voxel response by grouping at $[-12, -36, -12]$.

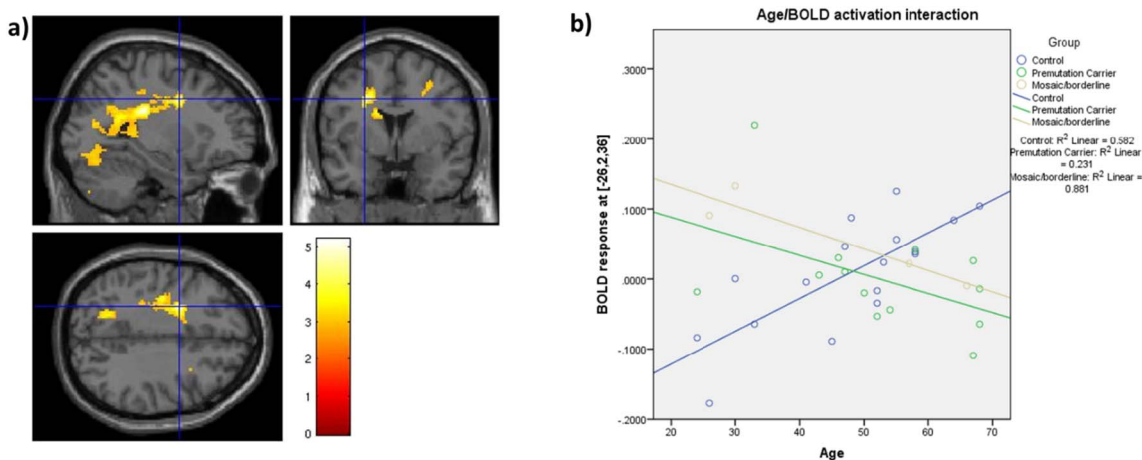


Fig. 3. Age-related between group imaging results a) Significant group \times age interaction ($FWE_{corr} < 0.001$, $T = 5.22$) at the left BA17, left hippocampus (CA), left inferior parietal cortex and left temporal in the sequential $>$ random condition contrast. Cluster co-ordinate of maximum voxel: $-26,2,36$, $k = 2105$, normalised voxel size: 2 mm^3 b) Fit linear regression lines comparing positive control BOLD response and age relationship compared to negative premutation carrier BOLD response and age relationship at maximum cluster voxel $[-26,2,36]$.

Table 2
Statistical results of within group regression analyses between participant age and BOLD activation at $[-26,2,36]$.

Within group age/BOLD activation regression analyses						
Group	DV	IV	β	Standard error	Adjusted R^2	p Value
Control	Age	BOLD response at $[-26,2,36]$	0.763	0.001	0.554	< 0.001
Premutation	Age	BOLD response at $[-26,2,36]$	-0.595	0.001	0.312	0.012

Borderline or mosaic carrier *FMR1* mRNA level relative to 18 sRNA and normalised to age-matched control show no significant differences compared to other carriers.

3.6. Linear regression analyses

Simple linear regression analyses were carried out on the imaging, clinical and *FMR1* mRNA variables of interest (Supplementary Fig. 1, Supplementary Table 2). Extracted raw voxel data from the cluster

global maxima originating from both the between group analysis and the group \times age interaction analysis were regressed against measures of tremor, co-ordination, balance and *FMR1* mRNA levels. No significant associations were identified in either carriers or controls (Supplementary Fig. 1a and 1b).

4. Discussion

This is the first study to examine brain activation during a motor task in *FMR1* premutation carriers who do not have frank symptoms of FXTAS. Consistent with the primary hypothesis, despite the lack of clinical symptomatology, differences between carriers and controls were identified when contrasting random and sequential finger-tapping conditions in this fMRI task in the bilateral lobules VI of the cerebellum, left lobule V and the left hippocampus (subiculum).

The cerebellum is a brain region which is strongly associated with movement initiation and processing, as well as being a site of degeneration in FXTAS (Berry-Kravis et al., 2007). We now show a pre-symptomatic functional BOLD response alteration in the cerebellum, extending into the hippocampus, during a finger-tapping task in a premutation population. Pertinently, recent evidence shows that carriers without FXTAS display a faster age-related decrease in cerebellar volume than controls. Significantly larger ventricles and significant group \times age interactions in the brainstem and whole brain volumes

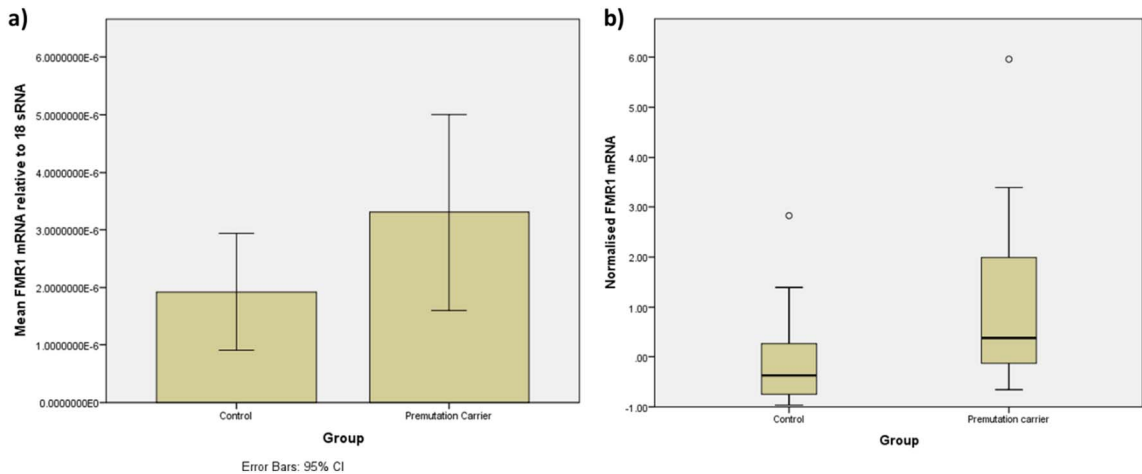


Fig. 4. *FMR1* mRNA quantification. a) *FMR1* mRNA amount relative to 18 sRNA control for carrier and control groups b) Carrier *FMR1* mRNA amount relative to 18 sRNA normalised to age-matched control levels and control *FMR1* mRNA amount relative to 18 sRNA normalised to control average.

were also identified in carriers without FXTAS (Wang et al., 2017). Sensorimotor mapping of the cerebellum labels lobule V of the cerebellum as primarily related to movements of the hand and finger-tapping tasks have previously been found to reliably activate cerebellar lobule V, with more cognitively demanding tasks also recruiting lobule VI (Stoodley et al., 2012; Grodd et al., 2001). Our finding of significantly lower activation at lobule VI of the cerebellum may well reflect deficits in recruitment during higher levels of demand during the task, in addition to a lower level of basic sensorimotor processing at lobule V. The hippocampus is not routinely cited as being significantly activated during within group analyses of fMRI motor tasks, however the extension of the significant between group cluster to the hippocampal subiculum may also indicate a deficit in more diffuse recruitment in response to a change in task demand (De Guio et al., 2012; Berns et al., 1999). This type of evidence of significant differences between carriers without FXTAS and controls during a motor task is suggestive of neurological vulnerability to disease prior to onset.

A significant group \times age interaction was also identified that revealed that, compared to controls, carriers showed a significantly more negative association between age and activation in the left BA17, left hippocampus (cornu ammonis), left inferior parietal cortex and left temporal lobe. Within group regression analysis of this data revealed that both the positive age-related correlation in the control group and the negative age-related correlation in the premutation group were significant. In normal elderly populations, finger-tapping has been seen to elicit over-recruitment of the occipito-temporo-parietal regions, suggesting an increased level of visual or mental strategizing (Zapparoli et al., 2013). This idea of compensatory activity is reflected in our regression analysis, with activation in the temporo-parietal cluster identified in this analysis showing a positive linear relationship with increasing age in the control population. However, this cluster shows significant deactivation in relation to age in the premutation group, suggesting that there is degeneration affecting the functional compensatory response to changes in movement demands.

In addition to imaging data, the present study utilized clinical measurements of tremor, co-ordination, balance and *FMR1* mRNA to further characterise the participant sample. Performance on the tremor and co-ordination measurements was significantly worse in carriers, suggesting subtle non-clinical symptoms. Balance however was not significantly different than in controls, and this may be explained by balance being affected later on during FXTAS progression, as falls are not often reported in early disease stages, meaning that balance symptomatology is not present in this asymptomatic or pre-clinical sample. None of these variables exhibited an association with the raw voxel data extracted from the between group analysis at the cluster at the bilateral lobules VI of the cerebellum, left lobule V and the left hippocampus (subiculum). It is possible in this case that a relatively small sample size for this study may have led to these results not reaching significance. Additionally, in the absence of overt FXTAS, it may be that symptomatology and functional brain changes are not yet developed enough to display a significant relationship, and a cross-sectional asymptomatic sample in this case may have led to a bias towards carriers with a lower FXTAS risk, especially in the older participants. Tremor, co-ordination and balance as measured by the CATSYS-2000 system also did not prove to be significantly associated with raw voxel data extracted from the age-related significant cluster at the left BA17, left hippocampus (cornu ammonis), left inferior parietal cortex and left temporal lobe. This may be due to the likelihood of this predominantly limbic cluster being more relevant to compensatory activity and motor imagery, instead of overt motor processing and associated deficits, in addition to the aforementioned limitations regarding power to detect a small effect size and the present study's cross-sectional design.

Measurements of *FMR1* mRNA from peripheral blood samples did not show any relationship with significant differences in BOLD response, in either the between group or age-related analysis. *FMR1*

mRNA levels are thought to be one of the primary molecular driving forces of neurodegenerative processes in FXTAS, and it is therefore somewhat surprising that *FMR1* mRNA amount is not related to these functional imaging changes. Our findings contrast with previous studies that support the hypothesis that early signs of brain changes associated with FXTAS correlate with changes in mRNA levels or metabolism (Cohen et al., 2006; Adams et al., 2007). These studies found that hippocampal volume and IQ scores were correlated with *FMR1* mRNA in premutation carriers. However, our findings are in agreement with other studies that found mRNA measurements from peripheral blood may be only weakly correlated with brain expression (Tassone et al., 2007; Cohen et al., 2006; Leehey et al., 2008). It is possible however that variation in asymptomatic premutation carrier populations in terms of future FXTAS penetrance may be a contributing factor to the discrepancies in the findings into *FMR1* mRNA levels in carriers. To elucidate this further, work in the field should attempt to strive towards methodology that can more directly identify molecular changes in the brain in vivo or post mortem.

Previous functional MRI research studies have also observed functional abnormalities in premutation carriers without FXTAS. During associative memory recall tasks, increases in activation at the parietal cortex is suggestive of compensatory mechanisms within premutation carrier groups, given that performance in the task was not significantly different to control subjects (Koldewyn et al., 2008). This type of neural compensation may be important in the carrier phenotype, allowing individuals to counteract processing deficiencies and appear outwardly asymptomatic. Findings of reduced activation in the limbic system of carriers is also further evidence of the higher incidences of social and psychiatric problems in carrier populations, and may indeed be linked to structural findings, such as volume loss at the amygdala (Hessl et al., 2011). Additionally, during a scanner task that involved the presentation of neutral faces to participants, premutation carriers were observed to respond to this type of stimuli with greater overall brain activation, which again may be reflective of social difficulties and neuropsychological abnormalities (Hessl et al., 2007). On the whole, fMRI in *FMR1* premutation carriers has shown a reduction in the BOLD signal at multiple different brain regions in response to varied stimuli. However, the literature is not without conflicting results, and some research groups have demonstrated no significant differences in comparison to control groups during functional testing (Wang et al., 2012). This absence of differences between groups may arise for many different reasons, one such important reason being that the heterogeneity of the premutation phenotype and percentage of FXTAS penetrance may cause studied groups of carriers to vary considerably. The present study however is consistent with the existence of altered BOLD response in carriers who do not show clinical signs of FXTAS.

Overall, we find novel results pertaining to motor function and response to variation in task demand using functional neuroimaging in Fragile X premutation carriers. Our results show brain changes in carriers in the cerebellar and limbic regions which are likely to reflect functional impairment of compensatory mechanisms and response to increased task demand. These changes pre-exist the diagnosis of FXTAS and are most marked in older carriers, suggesting that they may be indicative of FXTAS vulnerability. Future longitudinal studies are required to confirm this.

Funding

This work was funded by the RS MacDonald Trust and the Patrick Wild Centre through the Helen Maud-Garfit fund.

Appendix A. Supplementary data

Supplementary data to this article can be found online at <https://doi.org/10.1016/j.nicl.2017.12.016>.

References

- Adams, J.S., et al., 2007. Volumetric brain changes in females with fragile X-associated tremor/ataxia syndrome (FXTAS). *Neurology* 69 (9), 851–859. Available at: <http://www.ncbi.nlm.nih.gov/pubmed/17724287>, Accessed date: 30 April 2016.
- Adams, P.E., et al., 2010. Psychological symptoms correlate with reduced hippocampal volume in fragile X premutation carriers. *Am. J. Med. Genet. B. Neuropsychiatr. Genet.* 153B (3), 775–785. Available at: <http://www.ncbi.nlm.nih.gov/pubmed/19908235>, Accessed date: 30 April 2016.
- Aguiar, D., et al., 2008. A quantitative assessment of tremor and ataxia in FMR1 premutation carriers using CATSYS. *Am. J. Med. Genet. A* 146A (5), 629–635. Available at: <http://doi.wiley.com/10.1002/ajmg.a.32211>, Accessed date: 23 January 2017 (Accessed January 23, 2017).
- Allen, E.G., et al., 2008. Detection of early FXTAS motor symptoms using the CATSYS computerised neuromotor test battery. *J. Med. Genet.* 45 (5), 290–297. Available at: <http://jmg.bmj.com/cgi/doi/10.1136/jmg.2007.054676>, Accessed date: 6 January 2017.
- Bartenstein, P., et al., 1997. Central motor processing in Huntington's disease. A PET study. *Brain J. Neurol.* 1553–1567. Available at: <http://www.ncbi.nlm.nih.gov/pubmed/9313639>, Accessed date: 11 January 2017.
- Berns, G.S., Song, A.W., Mao, H., 1999. Continuous Functional Magnetic Resonance Imaging Reveals Dynamic Nonlinearities of “Dose–Response” Curves for Finger Opposition.
- Berry-Kravis, E., et al., 2007. Fragile X-associated tremor/ataxia syndrome: clinical features, genetics, and testing guidelines. *Movement Disorders: Official Journal of the Movement Disorder Society* 22 (14), 2018–2030. quiz 2140. Available at: <http://www.ncbi.nlm.nih.gov/pubmed/17618523>, Accessed date: 27 April 2016.
- Bourgeois, J.A., et al., 2007. Cognitive, anxiety and mood disorders in the fragile X-associated tremor/ataxia syndrome. *Gen. Hosp. Psychiatry* 29 (4), 349–356. Available at: <http://www.ncbi.nlm.nih.gov/pubmed/17591512>, Accessed date: 27 April 2016.
- Brown, S.S.G., Stanfield, A.C., 2015. Fragile X premutation carriers: a systematic review of neuroimaging findings. *J. Neurol. Sci.* 352 (1–2), 19–28.
- Brunberg, J.A., et al., 2002. Fragile X premutation carriers: characteristic MR imaging findings of adult male patients with progressive cerebellar and cognitive dysfunction. *AJNR Am. J. Neuroradiol.* 23 (10), 1757–1766. Available at: <http://www.ncbi.nlm.nih.gov/pubmed/12427636>, Accessed date: 29 April 2016.
- Cleary, J.D., Ranum, L.P.W., 2014. Repeat associated non-ATG (RAN) translation: new starts in microsatellite expansion disorders. *Curr. Opin. Genet. Dev.* 26, 6–15. Available at: <http://linkinghub.elsevier.com/retrieve/pii/S0959437X14000082>, Accessed date: 24 January 2017.
- Cohen, S., et al., 2006. Molecular and imaging correlates of the fragile X-associated tremor/ataxia syndrome. *Neurology* 67 (8), 1426–1431. Available at: <http://www.ncbi.nlm.nih.gov/pubmed/17060569>, Accessed date: 29 April 2016.
- Danish Product Development Ltd., 1988. CATSYS 2000 User's Manual.
- De Guio, F., et al., 2012. Functional magnetic resonance imaging study comparing rhythmic finger tapping in children and adults. *Pediatr. Neurol.* 46 (2), 94–100. Available at: <http://www.ncbi.nlm.nih.gov/pubmed/22264703>, Accessed date: 27 January 2017.
- Duarte, J.V., et al., 2016. Parametric fMRI of paced motor responses uncovers novel whole-brain imaging biomarkers in spinocerebellar ataxia type 3. *Hum. Brain Mapp.* 37 (10), 3656–3668. Available at: <http://www.ncbi.nlm.nih.gov/pubmed/27273236>, Accessed date: 11 January 2017.
- Filley, C.M., et al., 2015. White matter disease and cognitive impairment in FMR1 premutation carriers. *Neurology* 84 (21), 2146–2152. Available at: <http://www.ncbi.nlm.nih.gov/pubmed/25925982>, Accessed date: 29 December 2016.
- Garcia-Arocena, D., Hagerman, P.J., 2010. Advances in understanding the molecular basis of FXTAS. *Hum. Mol. Genet.* 19 (R1), R83–9. Available at: <http://www.ncbi.nlm.nih.gov/pubmed/20430935>, Accessed date: 3 May 2016.
- Gountouna, V.-E., et al., 2010. Functional Magnetic Resonance Imaging (fMRI) reproducibility and variance components across visits and scanning sites with a finger tapping task. *NeuroImage* 49 (1), 552–560. Available at: <http://www.ncbi.nlm.nih.gov/pubmed/19631757>, Accessed date: 23 January 2017.
- Grodd, W., et al., 2001. Sensorimotor mapping of the human cerebellum: fMRI evidence of somatotopic organization. *Hum. Brain Mapp.* 13 (2), 55–73. Available at: <https://doi.org/10.1002/hbm.1025>, Accessed date: 27 January 2017.
- Hagerman, R., Hagerman, P., 2013. Advances in clinical and molecular understanding of the FMR1 premutation and fragile X-associated tremor/ataxia syndrome. *The Lancet Neurol.* 12 (8), 786–798. Available at: <http://www.ncbi.nlm.nih.gov/pubmed/23867198>, Accessed date: 27 April 2016.
- Hall, D.A., et al., 2005. Initial diagnoses given to persons with the fragile X associated tremor/ataxia syndrome (FXTAS). *Neurology* 65 (2), 299–301. Available at: <http://www.ncbi.nlm.nih.gov/pubmed/16043804>, Accessed date: 27 April 2016.
- Hall, D.A., et al., 2016. Update on the clinical, radiographic, and neurobehavioral manifestations in FXTAS and FMR1 premutation carriers. *Cerebellum* 15 (5), 578–586. Available at: <https://doi.org/10.1007/s12311-016-0799-4>, Accessed date: 29 December 2016 (Accessed December 29, 2016).
- Hashimoto, R., et al., 2011. Diffusion tensor imaging in male premutation carriers of the fragile X mental retardation gene. *Movement Disorders: Official Journal of the Movement Disorder Society* 26 (7), 1329–1336. Available at: <http://www.ncbi.nlm.nih.gov/pubmed/21484870>, Accessed date: 29 April 2016.
- Hessl, D., et al., 2007. Amygdala dysfunction in men with the fragile X premutation. *Brain J. Neurol.* 130 (Pt 2), 404–416. Available at: <http://www.ncbi.nlm.nih.gov/pubmed/17166860>, Accessed date: 29 April 2016.
- Hessl, D., et al., 2011. Decreased fragile X mental retardation protein expression underlies amygdala dysfunction in carriers of the fragile X premutation. *Biol. Psychiatry* 70 (9), 859–865. Available at: <http://www.ncbi.nlm.nih.gov/pubmed/21783174>, Accessed date: 29 April 2016.
- Jacquemont, S., et al., 2004. Penetrance of the fragile X-associated tremor/ataxia syndrome in a premutation carrier population. *JAMA* 291 (4), 460–469. Available at: <http://www.ncbi.nlm.nih.gov/pubmed/14747503>, Accessed date: 28 April 2016.
- Kim, S.-Y., et al., 2014. Altered neural activity in the “when” pathway during temporal processing in fragile X premutation carriers. *Behav. Brain Res.* 261, 240–248. Available at: <http://www.ncbi.nlm.nih.gov/pubmed/24398265>, Accessed date: 12 April 2017.
- Kloppel, S., et al., 2009. Functional compensation of motor function in pre-symptomatic Huntington's disease. *Brain* 132 (6), 1624–1632. Available at: <http://brain.oxfordjournals.org/cgi/doi/10.1093/brain/awp081>, Accessed date: 11 January 2017.
- Koldewyn, K., et al., 2008. Reduced hippocampal activation during recall is associated with elevated FMR1 mRNA and psychiatric symptoms in men with the fragile X Premutation. *Brain Imaging Behav.* 2 (2), 105–116. Available at: <http://www.ncbi.nlm.nih.gov/pubmed/19430586>, Accessed date: 29 April 2016.
- Leehey, M.A., et al., 2008. FMR1 CGG repeat length predicts motor dysfunction in premutation carriers. *Neurology* 70 (16 Pt 2), 1397–1402. Available at: <http://www.ncbi.nlm.nih.gov/pubmed/18057320>, Accessed date: 27 April 2016.
- Lewis, M.M., et al., 2011. Differential involvement of striato- and cerebello-thalamo-cortical pathways in tremor- and akinetic/rigid-predominant Parkinson's disease. *Neuroscience* 177, 230–239. Available at: <http://linkinghub.elsevier.com/retrieve/pii/S0306452210016994>, Accessed date: 11 January 2017.
- Li, Y., Jin, P., 2012. RNA-mediated neurodegeneration in fragile X-associated tremor/ataxia syndrome. *Brain Res.* 1462, 112–117. <http://www.ncbi.nlm.nih.gov/pubmed/22459047>, Accessed date: 3 May 2016.
- Loesch, D.Z., et al., 2005. Evidence for, and a spectrum of, neurological involvement in carriers of the fragile X pre-mutation: FXTAS and beyond. *Clin. Genet.* 67 (5), 412–417. Available at: <http://www.ncbi.nlm.nih.gov/pubmed/15811008>, Accessed date: 29 April 2016.
- Minkova, L., et al., 2015. Detection of motor changes in Huntington's disease using dynamic causal modeling. *Front. Hum. Neurosci.* 9, 634. Available at: <http://www.ncbi.nlm.nih.gov/pubmed/26635585>, Accessed date: 11 January 2017.
- Murta, T., et al., 2016. Phase-amplitude coupling and the BOLD signal: a simultaneous intracranial EEG (iEEG) - fMRI study in humans performing a finger-tapping task. *NeuroImage* 1 (146), 438–451. Available at: <http://www.ncbi.nlm.nih.gov/pubmed/27554531>, Accessed date: 12 January 2017.
- Rifé, M., et al., 2003. Incidence of fragile X in 5000 consecutive newborn males. *Genet. Test.* 7 (4), 339–343. Available at: <http://www.ncbi.nlm.nih.gov/pubmed/15000813>, Accessed date: 29 December 2016.
- Sorensen, P.L., et al., 2013. Newborn screening and cascade testing for FMR1 mutations. *Am. J. Med. Genet. A* 161A (1), 59–69. Available at: <http://www.ncbi.nlm.nih.gov/pubmed/23239591>, Accessed date: 29 August 2017 (Accessed August 29, 2017).
- Stoodley, C.J., Valera, E.M., Schmahmann, J.D., 2012. Functional topography of the cerebellum for motor and cognitive tasks: an fMRI study. *NeuroImage* 59 (2), 1560–1570. <http://www.ncbi.nlm.nih.gov/pubmed/21907811>, Accessed date: 27 January 2017.
- Tassone, F., Berry-Kravis, E.M., 2010. *The Fragile X-Associated Tremor Ataxia Syndrome (FXTAS)*. Springer, New York, NY.
- Tassone, F., et al., 2000. Elevated levels of FMR1 mRNA in carrier males: a new mechanism of involvement in the fragile-X syndrome. *Am. J. Hum. Genet.* 66 (1), 6–15. Available at: <http://www.ncbi.nlm.nih.gov/pubmed/10631132>, Accessed date: 3 May 2016 (Accessed May 3, 2016).
- Tassone, F., et al., 2007. CGG repeat length correlates with age of onset of motor signs of the fragile X-associated tremor/ataxia syndrome (FXTAS). *Am. J. Med. Genet. B. Neuropsychiatr. Genet.* 144B (4), 566–569. Available at: <http://www.ncbi.nlm.nih.gov/pubmed/17427188>, Accessed date: 27 April 2016.
- Wang, J.M., et al., 2012. Male carriers of the FMR1 premutation show altered hippocampal-prefrontal function during memory encoding. *Front. Hum. Neurosci.* 6, 297. Available at: <http://www.ncbi.nlm.nih.gov/pubmed/23115550>, Accessed date: 30 April 2016.
- Wang, J.Y., et al., 2013. Fragile X-associated tremor/ataxia syndrome. *JAMA Neurol.* 70 (8), 1022. Available at: <http://archneur.jamanetwork.com/article.aspx?doi=10.1001/jamaneurol.2013.2934>, Accessed date: 29 April 2016.
- Wang, J.Y., et al., 2017. Abnormal trajectories in cerebellum and brainstem volumes in carriers of the fragile X premutation. *Neurobiol. Aging* 55, 11–19. Available at: <http://linkinghub.elsevier.com/retrieve/pii/S0197458017300921>, Accessed date: 30 August 2017.
- Zapparoli, L., et al., 2013. Mental images across the adult lifespan: a behavioural and fMRI investigation of motor execution and motor imagery. *Exp. Brain Res.* 224 (4), 519–540. Available at: <http://link.springer.com/10.1007/s00221-012-3331-1>, Accessed date: 12 January 2017.